JOURNAL OF APPLIED ELECTROCHEMISTRY 14 (1984) 573–585

Electrochemical etching of titanium alloy castings

J. C. GRIESS, S. A. DAVID, R. J. GRAY

Oak Ridge National Laboratory, Oak Ridge, Tennessee 37830, USA

Received 10 November 1983

We used an electrochemical method to etch cast binary titanium alloys in an attempt to show their dendritic structures.Studies showed that when an alloy could be activated in either sulphuric, oxalic or fluosilicic acid, its anodic polarization curve had the same general shape and passivation potential for all alloys independent of alloying element or concentration. Consequently, in acid solutions, electrochemical etching was conducted at a constant potential slightly less noble than the passivation potential where the anodic current density was near the maximum. Of the alloys examined, only Ti–15%Cr was etchable in a concentrated caustic solution and etching occurred only in the transpassive potential region. Under our conditions we were able to show the dendritic structure in alloys containing 15%Cr, Ta, or Mo; at lower concentrations, or in the case of the 15%Nb alloy, the dissolution rates of the dendritic and interdendritic materials were too similar to differentiate between them on the etched surface.

1. Introduction

Because of their favorable strength-to-weight ratios and their corrosion resistance in many environments, titanium alloys are increasingly used in a variety of applications. Although much attention has been given to the properties of wrought alloys, less attention has been focused on castings and welds, specifically on the relationship between microstructure and mechanical properties. During solidification of alloys, the solid that first forms has a composition different from the melt from which it forms. Thus, the composition may vary from the dendrite core to the interdendritic region; this variation is referred to as microsegregation. Many factors affect the extent of microsegregation, such as the phase relations as given by the appropriate phase diagram, freezing rate and diffusion after solidification. The coarseness or fineness of a dendritic structure in a casting or a weld can both provide information about the cooling rate and influence the properties of the cast alloy.

To understand and characterize solidification behaviour and solute segregation in alloys, it is essential to delineate solidification substructure (dendrites). The usual method of determining the microstructure of a metal or alloy is to etch a polished specimen in an appropriate chemical reagent. If the compositional differences between the various phases of the alloy are such that different dissolution rates occur or if different crystallographic planes are attacked at different rates, the structure of the alloy can be deduced from the etched surface.

Since titanium and its alloys are resistant to many common reagents, they are usually etched in acid fluoride solutions to which an oxidizing agent, usually nitric acid, is added [1]. Such solutions have been only marginally successful in revealing dendritic structures in titanium alloys. Also, segregation-induced substructures are difficult to resolve in alpha–beta titanium alloy welds using conventional metallographic techniques due to post-solidification solid state transformation that commonly occurs in these alloys. Hence, an investigation was undertaken to reveal the solidification substructure in titanium alloys using potentiostatic etching.

Electrochemical studies have shown that in non-oxidizing acids (except hydrofluoric acid) the dissolution rate of titanium is increased by anodic polarization up to a given potential, specific to the environment, above which passivation occurs and the dissolution rate decreases to very low values [2, 3]. With some alloys the dissolution rate again increases at higher potentials (transpassivity) [4]. Thus, by controlling

the potential, it may be possible to selectively etch titanium alloys to bring out their microstructures. We could find no evidence that controlled potential etching has previously been used with either cast or wrought titanium alloys to determine their structure, but this technique has been successfully applied to the selective etching of phases in other alloys, examples of which are presented in References 5–8. Our purpose for this investigation was to determine whether the dendritic structure of titanium alloys could be delineated by the use of potentiostatic electrochemical methods.

2. Experimental procedures

About 60–100 g samples of binary titanium alloys of 1, 5 and 15 wt % Mo, Nb and Ta; 5 and 15 wt % Cr; and 5 wt % Al were arc melted and cast into buttons in a water-cooled copper hearth. In addition, a pure titanium button was prepared in the same manner. Each button had a diameter of 3–5 cm and a maximum thickness of about 1.7 cm. The buttons were cut across the centre, and from one of the halves two specimens were prepared: one for electrochemical polarization studies and another for metallographic polishing. The surfaces to be examined were usually parallel to the thickness of the button and extended from the bottom of the mould to the free surface. In two cases, however, the surface examined was transverse to the thickness of the casting.

Titanium wires were spot-welded to the electrochemical specimens on the side opposite that to be studied, and the test surfaces were polished on a 600 grit wheel. All other surfaces on the electrochemical specimens and the attached wires were coated with a stop-off lacquer. Exposed surface areas varied between 1 and 2 cm^2. Because of the irregular shape of the uncoated faces and the tendency of the lacquer to shrink and, in some cases, to become partially detached when the test solutions were hot, the exposed surface areas and consequently the calculated current densities were probably known to no better than about 25%.

The specimens to be polished metallographically were mounted in epoxy resin and polished through 0.5 μm diamond paste. In most cases these were chemically etched, but in others holes were drilled through the back of the epoxy mounts so that electrical contact could be made with the specimen. These latter specimens were electrolytically etched in specific electrolytes.

Only anodic polarizations were carried out with an AMEL model 551 potentiostat. Our usual procedure was to place the specimen in the test solution and wait until the open-circuit potential was stable for 10–15 min before we connected the specimen to the potentiostat. Starting from the open-circuit potential and proceeding in an anodic direction through the active–passive transition, the potential was increased in 10 mV increments. In this potential region, currents stabilized in 30 s or less, and currents were recorded between 30 and 60 s after each change in the potential. At potentials of about 100 mV more noble than the critical potential for passivation, the currents became small and continued to decrease for long periods. In this region the potential was increased in 50–200 mV increments up to +2.00 V with respect to a saturated calomel reference electrode (SCE); the currents were recorded 2–3 min after the potential was changed. Except for the Ti–15% Cr alloy, which exhibited transpassivity, the dissolution rate of the alloys in this potential range was too low to be of practical interest for etching. After reaching +2.00 V, the potential was incrementally decreased to the open-circuit potential. The fact that the polarization curves in the active dissolution range were essentially independent of the direction of polarization change indicated that adequate time had been allowed for current stabilization. However, in most cases when the electrolyte temperature was 80° C or above, shrinkage or partial loosening of the stop-off lacquer caused the exposed surface area to increase, and the 'apparent' current density was often somewhat greater on the reverse curve.

Potentiostatic rather than potentiodynamic techniques were used primarily because of the results reported by Gooch *et al.* [5] in experiments with stainless steel and because of the possible uncertainties in potentiodynamic methods as reported by Mansfeld [9].

All electrolyses except those in 10M KOH were conducted in a glass cell that contained a platinum counter-electrode separated from the cell with a porous frit, a Luggin capillary connected to an external SCE through a salt bridge, a gas sparging tube, a thermal regulator and the test specimen. In addition, the cell was equipped with a condenser

that had a water trap at the top, which prevented ingress of air to the cell. Nitrogen was sparged through the solution in the cell for 30 min before the specimen was introduced and then at a lower rate throughout the test. The cell was heated from the bottom with an infrared bulb, and the solution temperature was maintained to within ± 0.5° C of the desired temperature. The tests with 10M KOH were conducted in an open Teflon beaker at 88° C (190° F), and no attempt was made to shield the solution from air.

The tip of the Luggin capillary was 0.5–1 mm from the surface of the electode, and no correction was made for *IR* drop in the solution. The salt bridge connecting the reference electrode and the specimen was filled with 0.5M Na_2SO_4 in all cases; again, no corrections were made for liquid junction potentials or for thermal gradients in the salt bridge. Neglecting these corrections was justified because we were primarily interested in determining if the oxidation of selective parts of the alloys could be detected at specific potentials and not in a direct comparison of potentials in one system with those in another. All solutions were made from reagent-grade chemicals and demineralized water.

After an anodic polarization curve had been obtained, the specimen was examined microscopically. In most cases the specimen was then repolished and anodically polarized at a fixed potential in the active dissolution range and re-examined. In some cases the metallographically polished specimens were electrolysed and photographed after different periods.

Microcompositional differences across the surfaces of selected polished specimens were obtained with a JEOL 733 electron microprobe. The diameter of the electron beam in the scanning mode was 1 μm. The analysed width and depth are 1.5–2.5 times that diameter, depending on the excitation voltage, and are much smaller than the spacing between dendrites.

3. Results

3.1. *Anodic polarization curves*

Four different solutions were arbitrarily chosen as etchants: 5.5M (40%) H_2SO_4 at 80° C; boiling (104° C) 1M $H_2C_2O_4$; 0.5M H_2SiF_6 at room temperature (22–23° C); 10M (40%) KOH at 88° C. Figs. 1–3 show representative anodic polarization curves in each of the acid solutions. In these environments, the curves were similar in shape, and the potential at which the maximum current occurred was about the same for all alloys in each acid. Only the Ti–Cr alloys in 5.5M H_2SO_4 showed

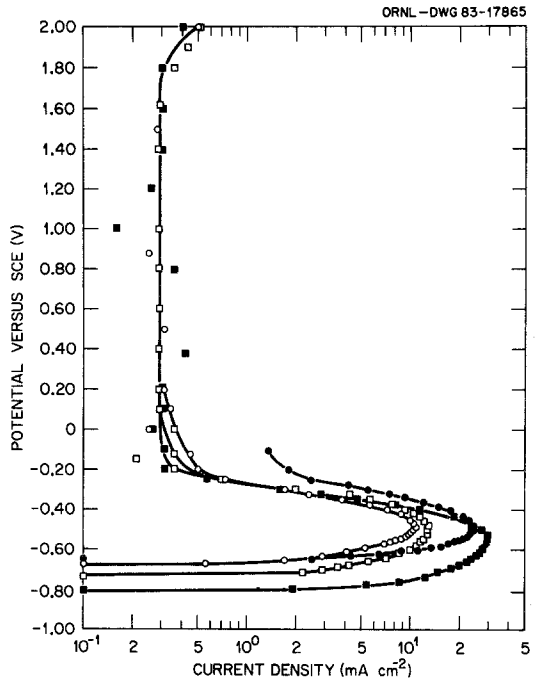

Fig. 1. Potentiostatic anodic polarization curves for four cast titanium alloys in 5.5M H_2SO_4 at 80° C. □ Ti–15% Ta; ○ Ti–15% Nb; ■ Ti–5% Cr; ● Ti–5% Ta.

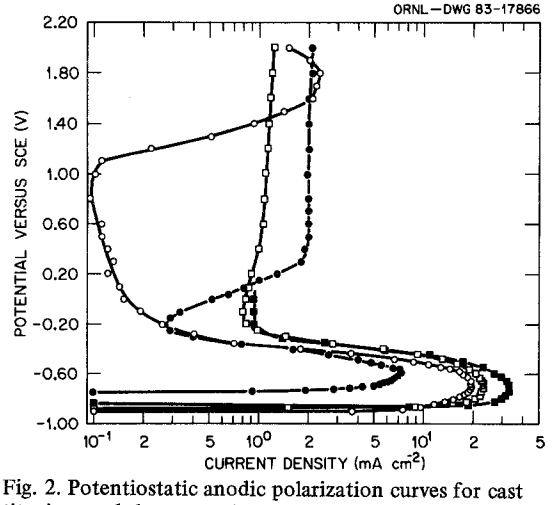

Fig. 2. Potentiostatic anodic polarization curves for cast titanium and three cast titanium alloys in 0.5M H_2SiF_6 at 23° C. ● Ti–15% Mo; ○ Ti–15% Cr; □ Ti–5% Al; ■ Ti.

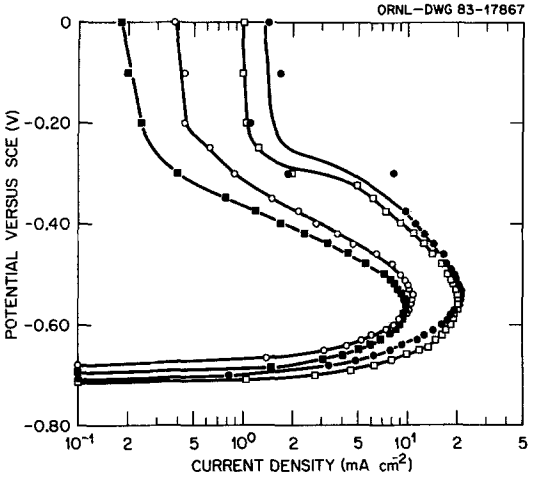

Fig. 3. Potentiostatic anodic polarization curves for cast titanium and three cast titanium alloys in 1M oxalic acid at 104° C. ○ Ti–15% Nb; ■ Ti–15% Ta; □ Ti–1% Ta; ● Ti.

evidence of transpassivity, and even in these cases there was no evidence of Cr(VI) formation; the current appeared to be primarily associated with the generation of oxygen.

Table 1 shows the maximum current densities and the corresponding potentials for the different cast alloys in acid solutions. The Ti–15% Mo alloy remained passive in both 5.5M H_2SO_4 and 1M $H_2C_2O_4$; for up to +2.00 V vs SCE the current densitities did not exceed a few tenths of a mA cm^{-2}. The data in Table 1 indicate that, with the Ti–Ta, Ti–Nb, Ti–Mo and Ti–Cr alloys, the maximum current density generally decreased as the alloy content increased. In all cases the shape of the anodic polarization curves of the alloys was similar to those obtained with pure titanium in acid solutions; that is, there were no irregularities that might indicate selective leaching of an element or of a specific phase from any of the alloys.

How the alloying elements fare during dissolution of the alloys in acid solutions is not completely clear. Chromium and aluminium are undoubtedly dissolved at potentials near or below the passivation potential of titanium and are soluble in the acids. Tantalum, niobium and molybdenum are passive in sulphuric acid and probably in oxalic acid, but thermodynamic data suggest that their inertness may be due to oxide films [10]. In any event, it appears unlikely that these elements would be soluble; consequently, they would probably remain on the surface of the corroding alloy, perhaps as metal but more likely as oxides. How these latter three elements behave in fluosilicic acid was uncertain, and anodic polarization curves were obtained with pure molybdenum and niobium in 0.5M H_2SiF_6. These curves are compared with that for cast titanium in Fig. 4. The open-circuit potentials for both elements were well above the passivation potential for titanium.

Table 1. Maximum anodic current density and corresponding potential for cast titanium alloys in three acid solutions

Alloying element (wt %)	5.5M H_2SO_4, 80° C		1M $H_2C_2O_4$, 104° C		0.5M H_2SiF_6, 23° C	
	Density (mA cm^{-2})	*Potential[a] (V)*	*Density (mA cm^{-2})*	*Potential (V)*	*Density (mA cm^{-2})*	*Potential (V)*
None	31	−0.50	21	−0.54	33	−0.73
1 Ta	33	−0.46	20	−0.55	32	−0.69
5 Ta	24	−0.49	13	−0.52	32	−0.68
15 Ta	13	−0.51	10	−0.57	25	−0.70
1 Nb	35	−0.46	25	−0.55	32	−0.67
5 Nb	18	−0.49	15	−0.54	26	−0.69
15 Nb	11	−0.49	11	−0.55	26	−0.69
1 Mo	37	−0.47	20	−0.55	35	−0.67
5 Mo	32	−0.48	8	−0.56	11	−0.61
15 Mo	0	−0.35[b]	0	−0.40[b]	7	−0.58
5 Cr	30	−0.56	18	−0.55	37	−0.73
15 Cr	45	−0.51	14	−0.61	16	−0.68
5 Al	47	−0.49	14	−0.56	23	−0.70

[a] Vs saturated calomel reference electrode.
[b] Value shown is open-circuit potential, which is above the potential at which passivity begins.

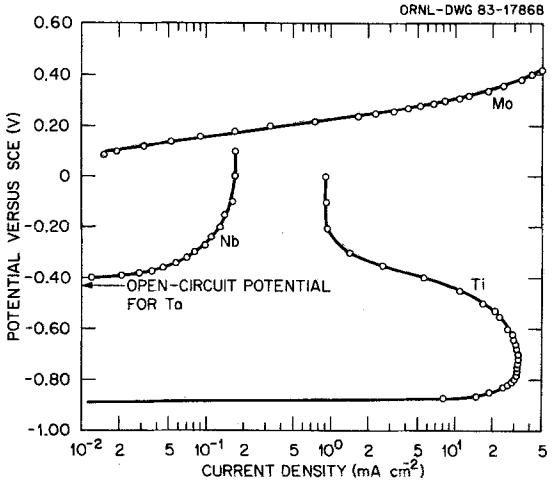

Fig. 4. Potentiostatic anodic polarization curves for titanium, niobium and molybdenum in 0.5M H_2SiF_6 at 23° C.

Molybdenum exhibited apparent transpassive behaviour, and after polarization the surface was covered with a powdery black deposit. Niobium was very polarizable and also developed a poorly adherent black film. Although an anodic polarization curve was not obtained with tantalum, its open-circuit potential was −0.43 V vs SCE (shown by arrow in Fig. 4), indicating that it was also noble to titanium in the active state.

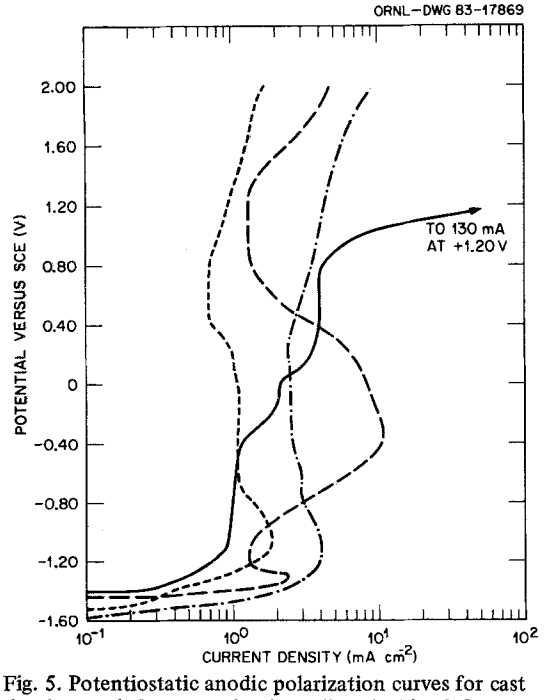

Fig. 5. Potentiostatic anodic polarization curves for cast titanium and three cast titanium alloys in 10M KOH at 88° C. —— Ti–15% Cr; — — — Ti–15% Mo; —·— Ti; – – – Ti–5% Al.

Preliminary tests showed that in 10M KOH at room temperature only very low current densities were achievable with the titanium alloys, and polarization curves were therefore obtained at the higher 88° C (190° F) temperature. Even at this temperature, current densities were relatively low and generally tended to drift with time to lower values. Fig. 5 shows the anodic polarization curves obtained with titanium and representative alloys. The data points have been eliminated for clarity. Had longer times been allowed between potential settings, lower current densities than shown would have resulted, except for the Ti–15% Cr alloy, where at potentials of about +1.0 V vs SCE the current densities increased with time. Examination of the Ti–15% Cr specimen electrolysed at potentials greater than +1.0 V vs SCE showed it to be free of any visible oxide and to have a selectively etched appearance. At these high potentials, a yellow colour characteristic of Cr(VI) developed in the solution, and TiO_2 could be observed falling from the surface. In addition, we observed oxygen evolution. On the other hand, all other alloys, including Ti–5% Cr, developed visible oxide films at all potentials greater than +1.0 V, and no signs of microstructure could be observed through the films. Interestingly, in the same solution at room temperature, an adherent oxide formed on Ti–15% Cr at potentials up to +5.0 V, and no Cr(VI) was produced in the solution.

Transpassive behaviour was observed in the Ti–15% Mo alloy, beginning at about −0.8 V vs SCE in the caustic solution. This behaviour was probably related to the oxidation of molybdenum in the film to some higher oxide. Once the surface molybdenum was oxidized, the current decreased in a manner similar to that observed with Ti–Mo alloys in hydrochloric acid solutions [4].

3.2. *Surface examination*

All the electrochemical specimens were examined microscopically after completion of the anodic polarization curve. In most cases the exposed surface was repolished and electrolysed at a fixed potential in the active dissolution potential region. In acid solutions this was usually about 25–50 mV less than the values shown in Table 1 but in one

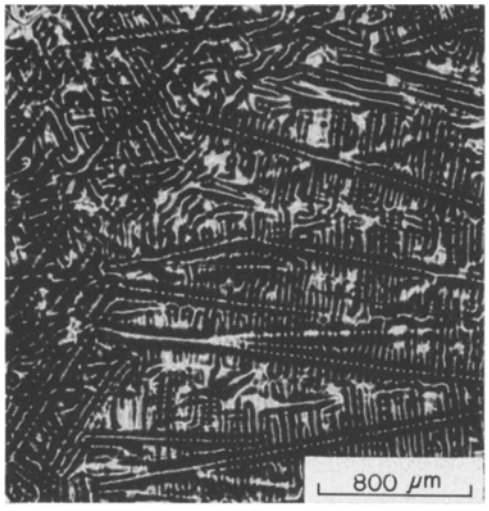

Fig. 6. Structure of the Ti–15% Cr casting after polarizing at +1.60 V vs SCE for 5 min in 10M KOH at 88° C. The surface is parallel to the cooling direction, and bright-field illumination was used.

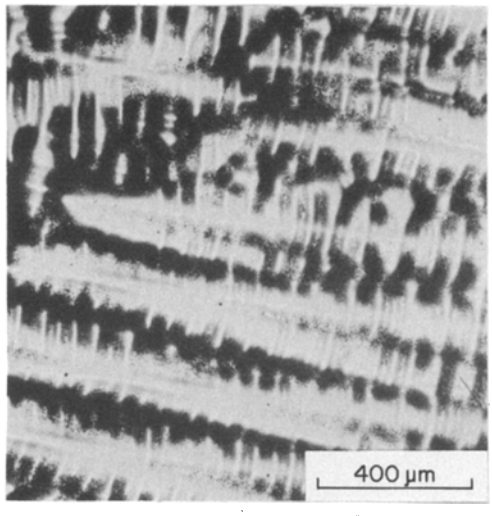

Fig. 7. Surface appearance of a Ti–15% Mo casting after polarizing at −0.58 V vs SCE in 0.5M H_2SiF_6 at 23° C for 10 min. The surface is parallel to the cooling direction and bright-field illumination was used.

case the potential was set at the current maximum. In addition, some of the metallographically polished specimens were potentiostatically etched.

Of all the alloys electrochemically etched, dendrites were observed on only three alloys: Ti–15% Cr, Ti–15% Mo, Ti–15% Ta. In the case of the Ti–15% Cr alloy, dendrites were only noticeable after etching at +1.0–2.0 V (and probably at higher potentials) in 10M KOH at 88° C. Fig. 6 is a low magnification photograph of a part of an etched specimen in which dendrites are clearly visible.

The surface shown in Fig. 6 was parallel to the cooling direction; that is, it had been cut through the thickness of the cast button. A surface was prepared transverse to the direction shown in Fig. 6 and electrolysed under the same conditions. The Cr(VI) formed as before, but at the end of the electrolysis the specimen was not bright, and dendrites were not detectable.

As indicated in Table 1, the Ti–15% Mo specimen could not be activated in either the sulphuric or oxalic acid solution, and transpassive behaviour was not noted in either of the solutions. In the fluosilicic acid solution Ti–15% Mo was active, and potentiostatic etching was carried out for 10 min at −0.58 V vs SCE. After electrolysis, dendrites were clearly evident, as illustrated in the bright-field photograph in Fig. 7. Similar results were obtained when the electrolysis was carried out at −0.62 V vs SCE. To illustrate the dendrites more clearly, the same specimen was photographed at a slightly lower magnification by an interference contrast technique (Fig. 8). Higher magnification examination showed that the arms of the dendrites protrude above the level of the interdendritic material. In comparison with Figs. 7 and 8, Fig. 9 shows bright-field and interference-contrast photographs, respectively, of a similar polished specimen that had been chemically

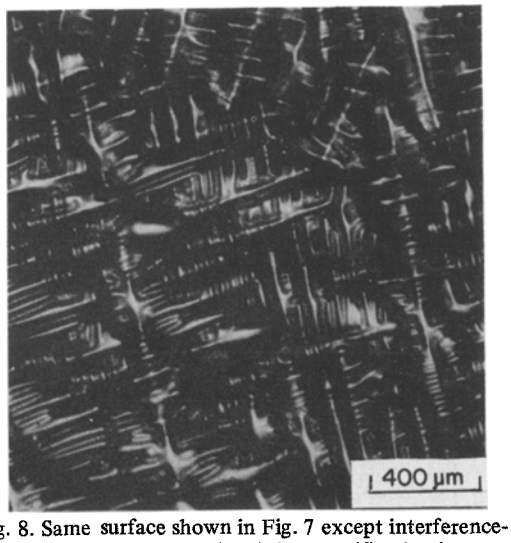

Fig. 8. Same surface shown in Fig. 7 except interference-constrast lighting was used and the magnification is slightly less.

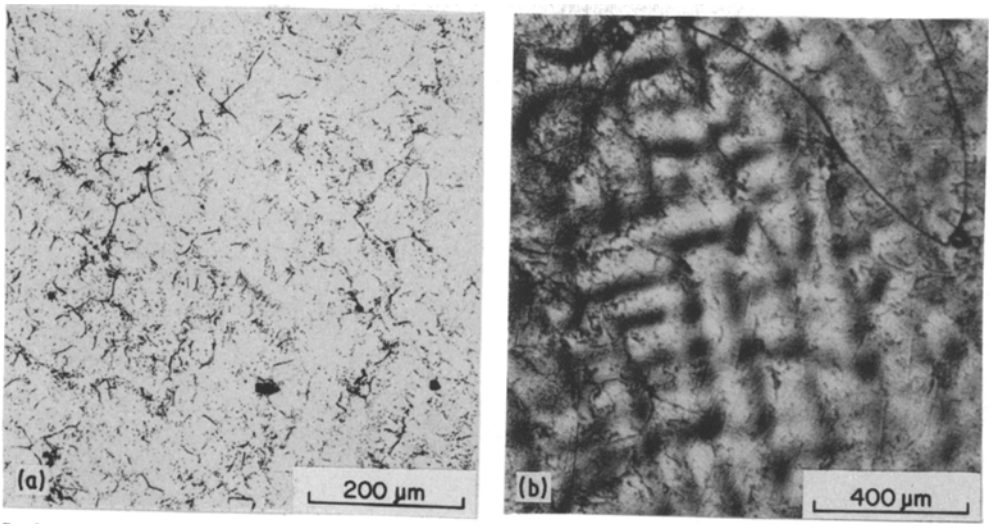

Fig. 9. Surface of Ti–15% Mo casting parallel to the cooling direction that was chemically etched in HNO_3–HF–lactic acid. (a) Bright-field illumination. Note that dendrites are not visible. (b) Interference-constant illumination. Dendrite structure is apparent but not nearly so clearly as in Figs. 7 and 8.

etched in an HNO_3–HF–lactic acid solution. The dendrites in the chemically polished specimen could be seen only by use of interference contrast, and then not very clearly.

A surface transverse to the direction shown in Figs. 7 and 8 was prepared and electrolysed under the same condition as previously. Fig. 10 shows the surface appearance after electrolysis. As in the case of the Ti–15% Cr alloy, dendrites were nearly absent; only faint suggestions of their presence were evident.

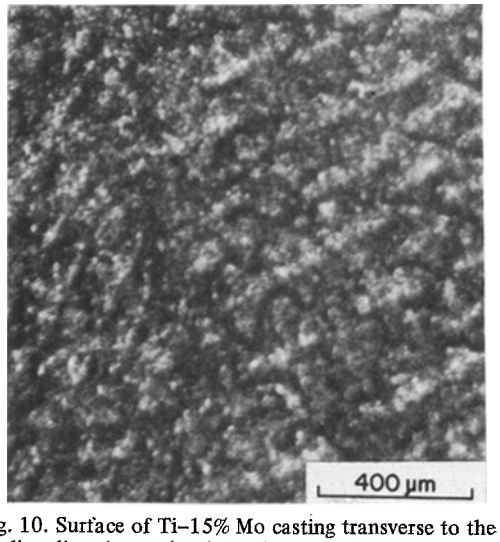

Fig. 10. Surface of Ti–15% Mo casting transverse to the cooling direction and polarized at −0.58 V vs SCE for 10 min in 0.5M H_2SiF_6 at 23° C. Bright-field illumination. Note the absence of clear-cut dendrites as observed when the surface was parallel to the cooling direction (Fig. 7).

An attempt to electroetch the Ti–5% Mo alloy to bring out the dendritic structure at −0.59 V vs SCE in fluosilicic acid was unsuccessful. Only uniform attack occurred. However, chemical etching of a metallographically polished specimen in an HNO_3–HF–lactic acid solution revealed dendrites at a few isolated locations on the surface (parallel to the cooling direction).

Both Ti–15% Cr and Ti–15% Mo specimens were heated in a vacuum furnace for 2 h at about 200° C below their melting points (1300 and 1525° C, respectively). Following the heat treatments the Ti–15% Cr alloy was electroetched in 10M KOH, and the Ti–15% Mo, in 0.5M H_2SiF_6. Both exposed faces were parallel to the cooling direction. During electrolysis of the Ti–15% Cr alloy, Cr(VI) formed, TiO_2 sloughed off the surface and the surface remained bright. However, examination showed only uniformly distributed micropits and no trace of dendrites. The Ti–15% Mo specimen underwent only uniform attack during electrolysis but had a uniform black film on its surface; no dendrites could be seen. The heat treatments redistributed the alloying elements to the extent that compositional differences between the dendrites and the rest of the material were too small to distinguish under our test conditions.

The Ti–15% Ta alloy was active in all three acids. After electrolysis at potentials of about 25 mV less noble than the passivation potential

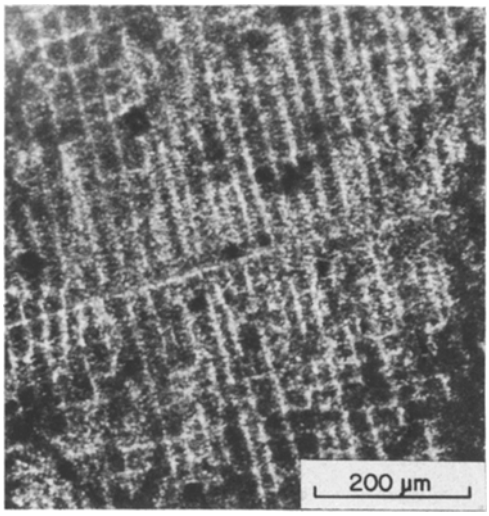

Fig. 11. Surface appearance of Ti–15% Ta casting in bright-field illumination after polarizing at −0.76 V vs SCE in 0.5M H_2SiF_6 for 45 min. Surface was parallel to cooling direction.

(shown in Table 1), dendrites could be observed over at least part of the surface. Fig. 11 shows the appearance of a specimen electrolysed in 0.5M H_2SiF_6 which was similar to those electrolysed in sulphuric and oxalic acids. In all three cases a film appeared to cover the surface and make the dendrites less distinct than in the other alloys. The film was white, but, considering the potential at which these electrolyses were carried out, TiO_2 should not have been on the surface. The composition of the film is unknown.

In the acid solutions, all alloys with 1% additions and those with 5% Al and 5 and 15% Cr behaved much like pure titanium in that, after electrolysis in the active region, the surface appeared to be free of any film and grain boundaries were clearly visible. However, no trace of dendrites could be found. Dark uniform films formed on the surfaces of alloys containing 5% Mo or Nb and 15% Nb. These films were easily wiped off with tissue paper, but, even after removal of the black film, significant microstructural features other than grain boundaries were not evident. In contrast, the 5% Ta alloy seemed to remain free of films during electrolysis.

3.3. *Surface analysis of polished specimens*

Compositional variations across the surface of several alloys are shown in Figs. 12–15. The dendrites on the polished surfaces of the tantalum, niobium and molybdenum alloys could be identified because of the differences in electron backscattering between titanium and the alloying element, and in these cases microprobe analyses were made across a single dendrite. The atomic numbers of titanium and chromium are so close that dendrites could not be distinguished in the Ti–15% Cr alloy, and a scan of 225 μm was arbitrarily made. In all cases readings were taken at 5 μm intervals.

In the case of the 15% Ta, Nb and Mo alloys, clear evidence of the increased concentration of the alloying elements in the dendrite core can be seen. For these alloys the ratios of the highest alloying element concentration to the lowest (segregation ratios) were 1.25, 1.20 and 1.25, respectively. For the 5% Ta alloy a well-defined increase in tantalum within the dendrite core was observed, and the segregation ratio was about 1.30. On the other hand, in the 5% Mo alloy the increased concentration of molybdenum within the dendrite seemed to extend over a wider range than in the Ti–15% Mo alloy, and the ratio was only 1.17. In the Ti–15% Cr alloy the segregation ratio was only 1.16. In contrast with the other alloys, in which the dendrites were richer in the alloying element than that in the interdendritic material, the cooling curve for Ti–Cr alloy is such that the higher chromium content should be in the interdendritic material [11]. By virtue of etching in the transpassive region the chromium-rich material was selectively removed so that the dendrites stood above the interdendritic material.

4. Discussion

We have attempted to use electrochemical polarization to define potentials at which it may be possible to selectively etch titanium alloy castings to reveal their dendritic structure. We could find no reported electrochemical investigation of cast titanium alloys in acid solutions, and a comparison of our electrochemical results with those obtained with similar wrought alloys is of interest. With our cast alloys in 5.5M H_2SO_4 the maximum current decreased as the alloy content increased, except for the Ti–Cr alloys, for which the maximum current was greater with 15% Cr than with 5% Cr. In oxalic acid the maximum current density for

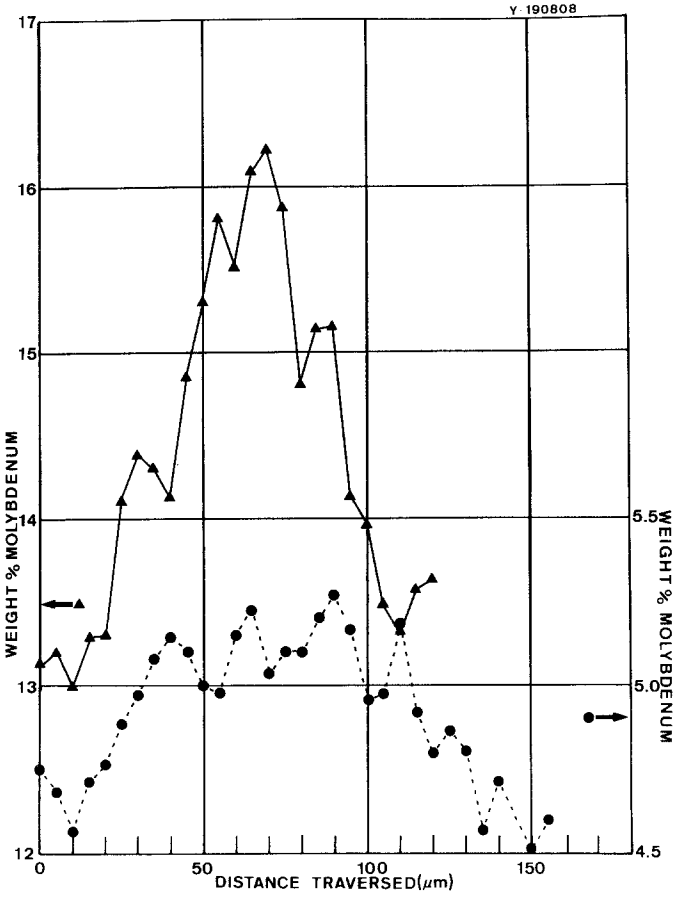

Fig. 12. Variation in molybdenum concentration in a Ti–Mo castings. ▲ Ti–15% Mo; ● Ti–5% Mo.

all alloy systems, including Ti–Cr, decreased as the alloy content increased. On the other hand, the maximum current densities in fluosilicic acid changed only slightly in going from the 1–15% alloys of tantalum and niobium, but, for the molybdenum and chromium alloys, the current decreased as the alloy content increased.

In cast alloys the alloying elements are not homogeneously distributed (i.e. dendrites and interdendritic material differ in composition), and the maximum current densities presented in Table 1 represent oxidation rates averaged over the surface. Few results for wrought binary titanium alloys of similar composition, in which the alloying element is more nearly homogeneously distributed, have been reported. Tomashov *et al.* [12] tested wrought titanium alloys with 1–8% Nb, 0.4–5% Mo and 0.3–5% Cr in 5.5M H_2SO_4 at 80° C. Of particular interest was the fact that, in the case of the Ti–Nb alloys, a change in niobium content from 4–8% resulted in a maximum current density change from 19 to 16 mA cm^{-2}; with the Ti–Mo system, increasing the molybdenum content from 3 to 5% decreased the current density only from 9.4 to 8.1 mA cm^{-2}. As far as comparisons could be made, our results were generally in agreement with theirs, although in all cases their maximum current densities were somewhat lower than were ours. It is not clear whether our higher values were due to the as-cast structure or to degradation of the stop-off lacquer, which increased the exposed area and resulted in higher apparent current densities. In any event, the effect of alloying content was the same in both studies, including the increase in maximum current density with the increased chromium concentration. Also in agreement with our results, Tomashov *et al.* noted that in 5.5M H_2SO_4 the potential at the current maximum was practically unaffected by the nature or concentration of the alloying element [12]. Our results show that the same observation is true in both oxalic and fluosilicic

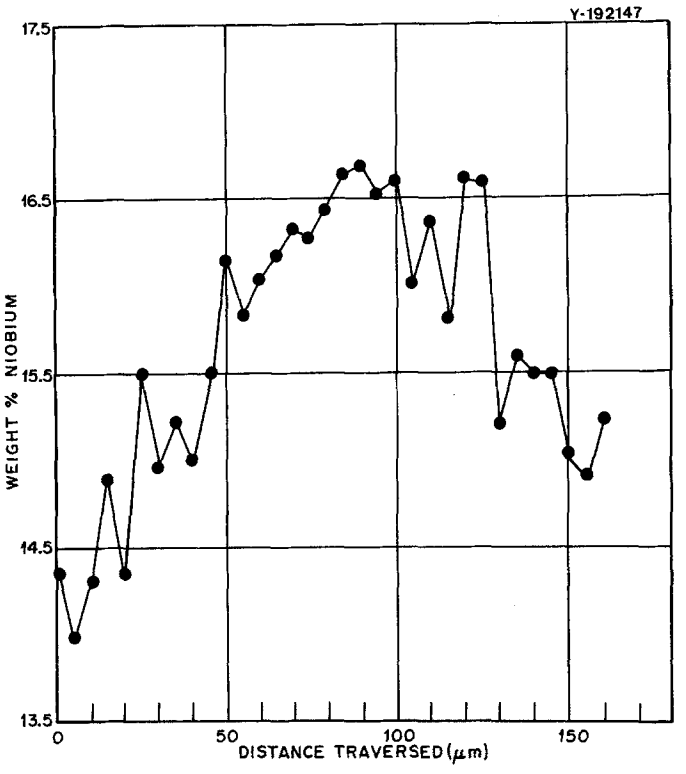

Fig. 13. Variation in niobium concentration in a Ti–15% Nb casting.

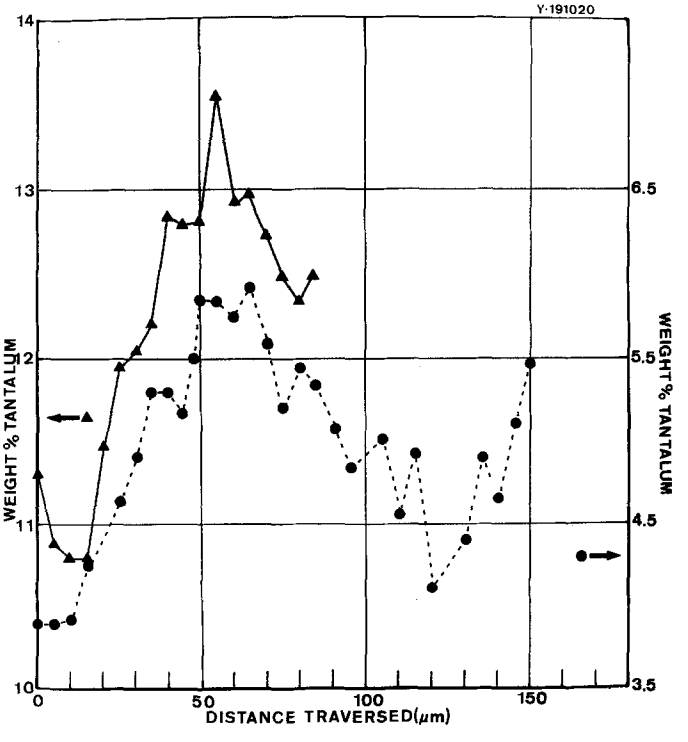

Fig. 14. Variation in tantalum concentration in Ti–Ta castings. ▲ Ti–15 wt % Ta; ● Ti–5 wt % Ta.

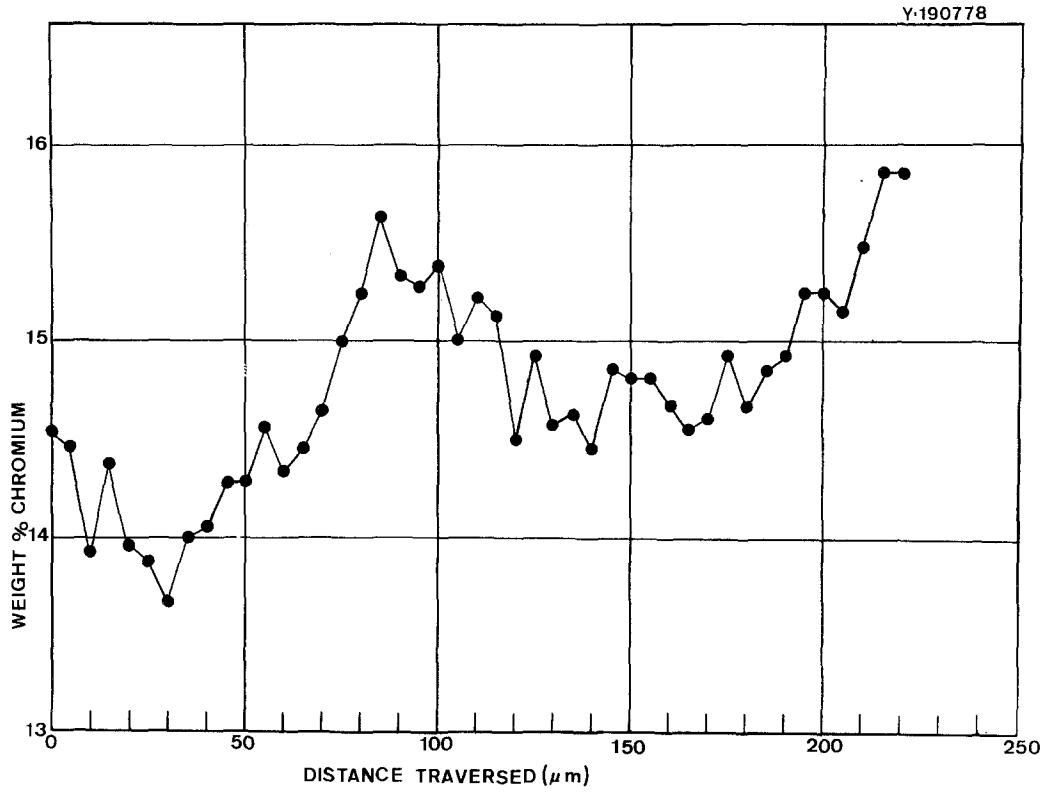

Fig. 15. Variation in chromium concentration in a Ti–15% Cr casting.

acids and indicate that the development of passivity results from the formation of TiO_2 films.

In another paper, Tomashov *et al.* [13] reported on the corrosion of forged and heat-treated Ti–Nb and Ti–Ta alloys in 5% HCl. They noted that the corrosion rate decreased slowly as the alloy content increased, but at about 15–20% Ta and 20–25% Nb large drops in corrosion rates, a factor of 10 or more, were observed.

Studies with forged Ti–Mo alloys in boiling 1M HCl showed that, as the molybdenum content increased, the critical current density for passivation decreased until at 20% Mo it was impossible to activate the alloy [4]. Peters and Myers [14] studied the behaviour of commercial purity titanium and several commercial alloys in sulphuric acid solutions at room temperature. They concluded that the critical current density for passivation was independent of composition. The alloy content was not varied systematically, and it is probably fortuitous that the alloys they used had similar critical current densities.

Thus, although detailed comparisons of our results with those of others were impossible, the available data suggest that the electrochemical behaviour of cast alloys is not greatly different from that of corresponding wrought alloys and that in most cases the corrosion rate of a given alloy system decreases as the concentration of the alloying element increases. However, the corrosion rate does not decrease linearly with alloy content.

Our studies showed that the alloys that could be activated had only one active dissolution potential range in acid solutions. In a given acid, the shapes of the anodic polarization curves were similar for all alloys and the potential at which the maximum current occurred was independent of alloying element or concentration. Therefore, we attempted to develop the dendritic structure in acid solutions at potentials slightly less than that at the current density maximum. Only the Ti–15% Cr alloy underwent significant dissolution in caustic solution, which occurred in the transpassive potential range.

To show dendrites in a cast alloy by either chemical or electrochemical etching, the composition difference or crystallographic orientation between the dendrites and interdendritic material

must be such that the dissolution rate of the dendrites is either significantly higher or lower than that of the interdendritic material. Electron microprobe analysis showed that the Mo, Ta, Nb and Cr alloys (only alloys examined) had detectable compositional differences between the dendrites and the interdendritic material. In fact, with the Ti–Mo alloys the segregation ratio agreed well with the results of Nurminen and Brody [15]. We were unable to find similar comparison data for the other alloys, but our results show that the segregation ratios were about the same as those for molybdenum. The segregation ratios in the Ti–Ta and Ti–Mo alloys were not greatly different between the 5 and 15% alloys.

The question might then be asked, why in acid solution could the dendrites be brought out electrochemically in the 15% alloys of tantalum and molybdenum and not at the lower concentrations nor in any of the niobium alloys? The answer to that question is suggested by the results of Tomashov *et al.* [13], who showed that in acid solutions the rate of change of oxidation rate with concentration of tantalum in titanium alloys is at or near a maximum at about 15%. In a similar environment other data indicate that with Ti–Mo alloys the greatest change in oxidation rate also occurs somewhere between 10 and 20% [4]. Furthermore, our data and those of others indicate that titanium and its alloys behave about the same in any acid solution. Thus, the corrosion rate of the Ti–15% Mo alloy in fluosilicic acid clearly differs significantly between the dendrites and the interdendritic material, even though the difference in molybdenum concentration is not large (13–16%). Similar results, although not as clear, were noted for Ti–15% Ta. Based on the data of Tomashov *et al.* [13] for Ti–Ta and Ti–Nb, the difference in corrosion rate between, for example, a 4 and 5% alloy of tantalum is much less than between a 12 and 15% alloy. In the former case it would not be possible to observe dendrites by chemical or electrochemical etching, whereas in the latter case it should be possible. It should be noted that this observation applies to strong acid solutions and that results might be different in other environments.

The data of Tomashov *et al.* [13] also explain why we could not bring out the dendritic structure in the Ti–Nb alloys. They showed that the maximum change in oxidation rate of these alloys occurs at about 20% Nb and that in the range from 14.5 to 16.5% Nb oxidation (interdendritic and dendritic, respectfully) rates are too close to allow delineation of the dendrites. Their data suggest that, at an average niobium concentration of about 20%, the dendrites could be brought out chemically or electrochemically.

Only in the case of the Ti–15% Cr alloy could we observe clear-cut transpassive behaviour, and this was only observed in hot 10M KOH solution. In this case Cr(VI) formed in solution, and dendrites were clearly visible after electrolysis at high potential. The interdendritic material was rich in chromium, and the dendrites were rich in titanium. In view of the fact that the Ti–5% Cr alloy did not show transpassive behaviour but only developed an oxide film, one must conclude that some minimum chromium concentration is needed to allow continuous oxidation of chromium from the alloy. At low concentrations only TiO_2 formed. The Ti–15% Mo alloy seemed to show transpassive behaviour in the alkaline solution, but this must have been related to oxidation of molybdenum from an existing oxide without significant attack on the substrate. After electrolysis the specimen was coated with an oxide and showed no selective etching.

5. Summary

Using a potentiostat, we were able to show the dendritic structure of the binary titanium alloys containing 15% Mo, 15% Cr and 15% Ta. In the Ti–15% Mo and Ti–15% Ta alloys, the interdendritic material was preferentially removed in acid solution, leaving the alloy-rich dendrites in relief. With the Ti–15% Cr alloy the chromium-rich interdendritic material was removed in the transpassive potential region in a strong caustic solution. It should be noted that electrochemical etching more clearly delineated the dendritic structure than chemical etching.

At lower alloy concentrations in the same systems, and in the Nb and Al alloys, the difference in dissolution rates between the dendrites and interdendritic material was too small to differentiate between the two regions. In different solutions, or perhaps even at different concentrations and temperatures of the same solutions

that we used, it may be possible to achieve sufficiently different rates to permit observation of the dendritic structure in these alloys.

Acknowledgements

This research was sponsored with support from the Office of Naval Research under interagency agreement with DOE 40-1206-81, Navy N00014-83-F-0020 and by the two exploratory studies programs at the Oak Ridge National Laboratory under Union Carbide Contract W-7405-eng-26 with the US Department of Energy.

This article is published by the kind permission of the US Government.

References

[1] H. R. Odgen and F. C. Holden, 'Metallography of Titanium Alloys, TML-103', Titanium Metallurgical Laboratory, Battelle Memorial Institute, Columbus, Ohio, 29 May, 1958, Appendix C.
[2] M. Stern and H. Wissenberg, *J. Electrochem. Soc.* **106** (1969) 755.
[3] N. D. Tomashov, R. M. Altovsky and G. P. Chernova, *ibid.* **108** (1961) 113.
[4] J. C. Griess, *Corros.* **24** (1968) 96.
[5] T. G. Gooch, J. Honeycomb and P. Walker, *Brit. Corros. J.* **6** (1971) 148.
[6] C. Edeleanu, *J. Iron Steel Inst.* **185** (1957) 482.
[7] Y. M. Kolotyrkin, L. M. Nerodenko and L. N. Yagupol'skaya, *Ind. Lab.* **38** (1972) 357.
[8] H. Hughes, *J. Iron Steel Inst.* **204** (1966) 804.
[9] F. Mansfeld, *Corros.* **38** (1982) 556.
[10] M. Pourbaix, 'Atlas of Electrochemical Equilibria in Aqueous Solutions', 2nd ed., National Association of Corrosion Engineers, Houston, Texas, and Cebelcor, Brussels (1974).
[11] A. D. McQuillan and M. K. McQuillan, 'Titanium', Academic Press, New York (1956).
[12] N. D. Tomashov, Yu. S. Ruskol, G. A. Ayuyan, Yu. M. Ivanov, G. M. Plavnik and R. I. Nazarova, *Prot. Metal.* **9** (1973) 7.
[13] N. D. Tomashov, T. V. Chukalovskaya, G. P. Chernova, P. B. Budberg and A. L. Gavze, *ibid.* **8** (1972) 1.
[14] J. M. Peters and J. R. Myers, *Corros.* **23** (1967) 326.
[15] J. I. Nurminen and H. D. Brody in 'Titanium Science and Technology, Proceedings of 2nd International Conference, 1972', Vol. 3, edited by R. I. Jaffee, Plenum Press, New York (1973).